HHS Public Access

Author manuscript

Exp Eye Res. Author manuscript; available in PMC 2016 October 01.

Published in final edited form as:

Exp Eye Res. 2015 October ; 139: 97–107. doi:10.1016/j.exer.2015.07.018.

Hyaluronan cable formation by ocular trabecular meshwork cells

Ying Ying Sun and **Kate E. Keller**[1]

Abstract

Hyaluronan (HA) in the ocular trabecular meshwork (TM) is a critical modulator of aqueous humor outflow. Individual HA strands in the pericellular matrix can coalesce to form cable-like structures, which have different functional properties. Here, we investigated HA structural configuration by TM cells in response to various stimuli known to stimulate extracellular matrix (ECM) remodeling. In addition, the effects of HA cable induction on aqueous outflow resistance was determined. Primary TM cell cultures grown on tissue culture-treated plastic were treated for 12–48 hours with TNFα, IL-1α, or TGFβ2. TM cells grown on silicone membranes were subject to mechanical stretch, which induces synthesis and activation of ECM proteolytic enzymes. HA structural configuration was investigated by HA binding protein (HAbp) staining and confocal microscopy. HAbp-labeled cables were induced by TNFα, TGFβ2 and mechanical stretch, but not by IL-1α. HA synthase (HAS) gene expression was quantitated by quantitative RT-PCR and HA concentration was measured by ELISA assay. By quantitative RT-PCR, HAS-1, -2, and -3 genes were differentially up-regulated and showed temporal differences in response to each treatment. HA concentration was increased in the media by TNFα, TGFβ2 and IL-1α, but mechanical stretch decreased pericellular HA concentrations. Immunofluorescence and Western immunoblotting were used to investigate the distribution and protein levels of the HA-binding proteins, tumor necrosis factor-stimulated gene-6 (TSG-6) and inter-α-inhibitor (IαI). Western immunoblotting showed that TSG-6 and IαI were increased by TNFα, TGFβ2 and IL-1α, but mechanical stretch reduced their levels. The underlying substrate appears to affect the identity of IαI•TSG-6•HA complexes since different complexes were detected when TM cells were grown on a silicone substrate compared to a rigid plastic surface. Porcine anterior segments were perfused with 10 μg/ml polyinosinic:polycytidylic acid (polyI:C), a potent inducer of HA cables, and outflow rates were monitored for 72 hours. PolyI:C had no significant effect on outflow resistance in porcine anterior segments perfused at physiological pressure. Collectively, *HAS* gene expression, HA concentration and configuration are differentially modified in response to several treatments that induce ECM remodeling in TM cells. In ocular TM cells, our data suggests that the most important determinant of HA cable formation appears to be the ratio of HA chains produced by the different HAS genes. However, the act of rearranging pericellular HA into cable-like structures does not appear to influence aqueous outflow resistance.

[1]Corresponding author: Kate E. Keller, Casey Eye Institute, Oregon Health & Science, University, 3181 SW Sam Jackson Park Rd, Portland, OR, 97239. Phone: (503) 494 2366, Fax: (503) 418 2399, gregorka@ohsu.edu.

Disclosure: Y. Sun, none; K. Keller, none.

Keywords

glaucoma; trabecular meshwork; extracellular matrix; hyaluronan; aqueous outflow

Hyaluronan (HA) is a large, negatively charged glycosaminoglycan (GAG) chain that is composed of repeating disaccharide units of glucuronic acid and N-acetylglucosamine. (Toole, 2004) The final HA chain can range from 2,000 to 25,000 disaccharide units in length. HA is synthesized by three related hyaluronan synthase (HAS) enzymes called HAS1, HAS2 and HAS3.(Itano et al., 1999) These HASs are located at the cell membrane. The activity of each HAS gene directly correlates to the size and amount of HA synthesized. HAS2 produces abundant high molecular weight (MW) HA, HAS1 produces small amounts of high MW HA, while HAS3 synthesizes low MW HA, but in large amounts.(Itano et al., 1999) Newly synthesized HA is extruded directly from the cell into the extracellular matrix (ECM). Once it is secreted, HA can remain tethered to the cell surface via receptors, which generates a voluminous cell-type specific pericellular matrix that influences various properties of the cell.(Toole, 2004) Pericellular HA can inhibit ligand access to receptors, limit phagocytosis and cause cell cycle arrest.(Stern et al., 2006)

Two configurations of HA have been described: globular HA, which is the classical form detected in the pericellular matrix, and HA cable-like structures. HA cable formation was first described in intestinal mucosal smooth muscle cells treated with the viral mimetic, polyinosinic-polycytidylic acid (polyI:C).(de la Motte et al., 2003) HA cables have subsequently been detected in several other cell types including proximal tubular epithelial cells, epidermal keratinocytes, fibroblasts, and airway smooth muscle cells.(Evanko et al., 2009; Jokela et al., 2008; Lauer et al., 2009; Selbi et al., 2006b) HA cables typically arise from the peri-Golgi and individual HA strands become cross-linked and complexed into HA cables.(Day and de la Motte, 2005) HA cables appear to function as scaffolds, which could prevent loss of ECM components during tissue remodeling or act as a template for matrix regeneration.(Evanko et al., 2009) The biological properties of HA cables differs from that of pericellular HA since cables are adhesive for leukocytes.(de la Motte et al., 2003) Thus, HA cables have a unique architecture and different functional activities than pericellular globular HA.

Little is known about the biological processes involved in HA cable formation. Previously, it was suggested that HA cable formation was a self-contained latent response that was independent of protein synthesis since cycloheximide, a protein synthesis inhibitor, induced cable formation within 2–4 hours of treatment.(Hascall et al., 2004) Since then, several factors have been proposed to influence cable formation including modifying the activity of each HAS gene to alter the ratio of individual HA strands coalesced into the HA cable, increasing the number of cellular protrusions that could stabilize the cables as they assemble, altering pericellular matrix HA concentration, regulating the levels of ECM proteins that cross-link individual HA chains into cables, or a combination of all these.(Day and de la Motte, 2005; Evanko et al., 2009; Kultti et al., 2006; Selbi et al., 2006b)

HA chains can be stabilized by numerous HA-binding proteins called hyaladherins.(Toole, 1990) A well-studied HA binding complex is that formed by inter-α-inhibitor (IαI).(Salier et

al., 1996; Zhuo et al., 2004) IαI is assembled in the Golgi apparatus and is composed of two heavy chains (HC1 and HC2) bound to the chondroitin sulfate chain of the proteoglycan, bikunin. (Zhao et al., 1995; Zhuo et al., 2004) IαI is a donor of HCs, which are enzymatically transferred to HA chains by an intermediary called tumor necrosis factor-stimulated gene-6 (TSG-6).(Milner et al., 2006) Transfer of HCs to HA chains is thought to stabilize the HA matrix since individual HA chains can be cross-linked into HA assemblies. (Milner et al., 2006; Toole, 2004) The proteoglycan, versican, is another hyaladherin that is associated with HA cables.(Evanko et al., 2009)

The trabecular meshwork (TM) in the anterior segment of the eye is the tissue responsible for establishing and maintaining intraocular pressure (IOP) within a normal range. Elevated IOP (> 22 mmHg), which is a primary risk factor for glaucoma, is caused by a blockage in the conventional aqueous humor outflow pathway in the TM.(Stamer and Acott, 2012) A normal homeostatic response to elevated IOP initiates degradation of the existing ECM by matrix metalloproteinases (MMPs).(Acott et al., 2014; Keller et al., 2009a) Concomitantly, deposition of new ECM facilitates the egress of aqueous humor from the anterior chamber, which in turn reduces elevated IOP. The role of HA in the regulation of IOP was first demonstrated in the 1950s.(Barany and Scotchbrook, 1954; Francois et al., 1956) Since then, other studies have shown that enzymatic degradation of HA by hyaluronidases increases outflow in some, but not all, animal species.(Grant, 1963; Hubbard et al., 1997; Keller et al., 2008; Knepper et al., 1984; Sawaguchi et al., 1993) Furthermore, HA concentration was lower in glaucoma TM than age-matched controls.(Knepper et al., 1996a) Our most recent data demonstrated that RNAi silencing of *HAS1* and *HAS2* genes decreased HA concentration and reduced outflow through the human TM.(Keller et al., 2012b) Thus, several lines of evidence point toward HA concentration as an important factor in aqueous outflow.

Various stimuli are known to increase or reduce aqueous outflow through the TM by inducing ECM remodeling. For instance, mechanical stretch, which mimics the stretch and distortion that is placed on TM cells *in situ* during pressure fluctuations, induces secretion and activation of MMPs.(Bradley et al., 2001) Additionally, the inflammatory cytokines, tumor necrosis factor-α (TNFα) and interleukin-1α (IL-1α), are released following laser trabeculoplasty, a common surgical treatment for glaucoma patients.(Bradley et al., 2000) Application of these cytokines to anterior segment perfusion culture increased outflow rates. (Bradley et al., 2006) Conversely, transforming growth factor-β2 (TGFβ2), levels of which are increased in the aqueous humor of glaucoma patients,(Fleenor et al., 2006; Gottanka et al., 2004; Inatani et al., 2001; Tripathi et al., 1994) decreased outflow in perfusion culture. However, it is not known how these external stimuli affect HA concentration or configuration in TM cells. Our main objectives of this study were to investigate whether HA cable-like structures are formed by ocular TM cells and to determine which factors appear to be important for HA cable formation. Results from this study will provide further insight into the role of HA in aqueous outflow resistance and in glaucoma.

Material and Methods

TM cell culture and treatments

Primary TM cell cultures were established from TM tissue dissected from 20 porcine eyes (Carlton Packing, Carlton, OR) as described previously.(Polansky et al., 1979; Stamer et al., 1995) All pieces of dissected TM tissue were placed in a T25 flask and cultured in Dulbecco's Modified Eagle's Medium (DMEM), 1:1 mixture of high and low glucose, containing 10% fetal bovine serum (FBS) and 1% penicillin-streptomycin-fungizone to allow the cells to populate the surface of the flask. When confluent, the mixed population of porcine TM cells was passaged to a maximum passage number of 5.

For cytokine treatments, cells were grown to confluence for at least 3 days in 6-well plastic tissue culture plates with serum-containing medium, washed with phosphate-buffered saline (PBS) and then placed into serum-free DMEM. The following cytokines were added: 10 ng/ml recombinant porcine TNFα, 10 ng/ml recombinant porcine IL-1α (R&D Systems, Minneapolis, MN), or 5 ng/ml activated TGFβ2 (Invitrogen, Carlsbad, CA). For mechanical stretch experiments, TM cells were cultured in 6-well FlexCell plates (BioFLex Int, Hillsborough, NC). These plates contain a flexible silicone elastomer membrane coated with collagen type I. Cells were grown to confluence, washed with PBS, placed into serum-free DMEM and a push pin was placed beneath the membrane of the well.(Bradley et al., 2001) A weight was applied to the lid of the plate, pushing the plate downward on the push pin and stretching the collagen-coated silicone membrane and attached cells. This produces a constant pressure with approximately 10% stretch/distortion.(Bradley et al., 2001)

Immunofluorescence and Confocal Microscopy

TM cells were plated on FlexCell membranes in serum-containing medium for at least 3 days, placed in serum-free medium and then treated with the cytokines and mechanical stretch for a further 3 days. Immunofluorescence and confocal microscopy were performed as detailed previously.(Keller et al., 2009b; Keller et al., 2008) Briefly, membranes were fixed in 4% paraformaldehyde and blocked in CAS universal blocking buffer (Invitrogen). In some experiments, ice-cold methanol or a mixture of acetic acid, ethanol and formalin was used to fix the cells as this better preserves HA structure.(Evanko et al., 2009) However, these fixatives were not used in all experiments as they destroyed epitope binding of the antibodies. Biotinylated hyaluronic acid-binding protein (bHAbp; EMD Biosciences, San Diego, CA) and Alexa Fluor 594-conjugated streptavidin was used to detect HA.(de la Motte and Drazba, 2011) The primary antibodies used were rabbit polyclonal anti-TSG-6 (Abcam, Cambridge, MA) and mouse polyclonal anti-IαI (AbFrontier, Seoul, South Korea). The appropriate species Alexa Fluor 488-conjugated secondary antibodies were used. Coverslips were mounted using ProLong gold mounting medium containing DAPI nuclear stain (Invitrogen). Images were captured using an Olympus Fluoview confocal microscope. Acquisition settings were identical for untreated and TNFα-treated TM cells. Open-source FIJI software (http://fiji.sc/Fiji) was used to stack the z-slices and process images post-capture.

Quantitative RT-PCR

RNA was isolated from TM cells treated for 12, 24 and 48 hours using cells-to-cDNA lysis buffer (Ambion, TX). cDNA was transcribed using Superscript III reverse transcriptase (Invitrogen). Quantitative RT-PCR was performed using HAS gene-specific primers (Table 1) and a Chromo4 PCR thermocycler (Biorad, Hercules, CA) with Opticon Monitor software (v3.1). The baseline was subtracted using the “cycles of the range” method and the amount of RNA was determined from a standard curve of known dilutions, which was generated for each primer set for every plate run. Data of each sample were normalized to 18S RNA, which acted as a house-keeping gene. Samples were run in duplicate from at least 3 independent experiments (see “n” listed in each figure legend). Data were then divided by control values, averaged and presented as a mean percentage of the control ± standard error of the mean.

HA concentration by ELISA assay

HA levels were quantitated using a sandwich ELISA assay (Echelon Bioscience, Salt Lake City, UT) as described previously.(Keller et al., 2012b) Briefly, TM cells were grown to confluence in serum-containing DMEM, washed with PBS and placed into serum-free DMEM. The cells were treated with the cytokines or mechanical stretch for a further 24 hours. At the end of the experiment, serum-free media was collected, while the cells and attached ECM were scraped into RIPA buffer on ice. The ELISA assay was performed according to the manufacturers’ directions. HA levels (ng/ml) were determined in triplicate from 100 μl of RIPA lysates and 100 μl serum-free media by comparing to HA standards that were run in tandem on each plate. HA concentration of the treated samples were divided by the control and made a percentage. Each percentage was then averaged and a standard error of the mean was calculated from 6 independent cell preparations.

Western immunoblotting

TM cells were grown to confluence, exchanged into serum-free media and treated with cytokines (plastic 6-well plates) or mechanical stretch (silicone membranes) for a further 48 hours. Serum-free media was collected and the total amount of protein in each sample was quantitated using a BCA protein assay (Pierce, Rockford, IL). Equal amounts of total protein were loaded on the gel and proteins were separated by SDSPAGE (BioRad Labs, Hercules, CA) under reducing conditions. Serum-free controls were run for both the rigid plastic surface and the silicone membrane. After protein transfer to nitrocellulose, membranes were blocked and then incubated with goat antibikunin (Santa Cruz Biotech, Inc, Dallas, TX) or rabbit anti-TSG-6 primary antibodies. Secondary antibodies were IRDye 700-conjugated anti-rabbit and IRDye 800-conjugated anti-goat (Rockland Immunochemicals, Gilbertsville, PA). Membranes were imaged on the Odyssey gel imaging system (Licor, Lincoln, NE). The intensity of each band was determined and experimental data are presented as a percentage of the untreated control. Results are representative of 3 independent experiments.

Poly(I:C) application to anterior segment perfusion culture

The viral mimetic, polyinosinic:polycytidylic acid (polyI:C), was used to induce cable formation.(de la Motte et al., 2003; Evanko et al., 2009) TM cells in culture were untreated

(control) or treated with 10 μg/ml polyI:C in PBS for 24 hours. HA cable induction was assessed using bHAbp, Alexa Fluor 594-conjugated streptavidin and confocal microscopy. Porcine anterior segments were perfused with serum-free media as described previously. (Keller et al., 2008; Keller et al., 2012b) Briefly, porcine eyes (Carlton Farms, Carlton, OR) were acquired within 4 hours of death and the anterior segment, devoid of the lens, iris and ciliary body, was placed onto the pedestal of a perfusion chamber. Anterior segments were perfused with serum-free DMEM at a constant pressure of 8 mmHg to give flow rates between 2 and 8 μl/min. Anterior segments that could not be stabilized were discarded. After flow rates had stabilized for 22 hours, polyI:C (10 μg/ml in PBS; Sigma Aldrich) was applied at time point 0. Control anterior segments were untreated. Outflow rates were monitored for a further 72 hours. Outflow rates for each individual anterior segment were normalized by dividing each data point after treatment by the average flow rate before treatment. Data were then averaged and a standard error of the mean was calculated for each time point.

Following perfusion, anterior segments were removed from the perfusion chambers and fixed in 4% paraformaldehyde. The tissues were embedded in paraffin and 5 μm radial sections were cut at the histopathology core facility of the Knight Cancer Institute (Oregon Health & Science University, Portland, OR).(Keller et al., 2008) Sections were deparaffinized, blocked and incubated overnight with bHAbp. Following washing, bHAbp was detected with Alexa Fluor 594-conjugated streptavidin. Sections were mounted in DAPI-containing mounting medium and images were acquired using a Fluoview laser confocal microscope.

Statistical Analyses

The number of replicates performed for each experiment is stated in the figure legends. Data are presented as the average ± standard error of the mean. Significance was determined using ANOVA. A $p < 0.05$ was considered statistically significant.

Results

HA configuration in TM cells

To investigate HA configuration in TM cells, we used biotinylated HA binding protein (HAbp), which is a link domain from aggrecan that binds HA with high affinity.(de la Motte and Drazba, 2011) In the pericellular matrix of untreated TM cells, HAbp labeled globular HA, which was visualized as punctate dots of variable size by confocal microscopy (Fig. 1A). TNFα treatment induced formation of long HA cable-like structures (Fig. 1B; arrows). HA cables were also apparent in TM cell cultures in response to TGFβ2 (Fig. 1C) and mechanical stretch (Fig. 1E). HA cables formed in response to mechanical stretch appeared to be slightly different as individual punctate dots appeared to align into cables rather than the more “solid” cables formed in than those formed in response to TNFα and TGFβ2 treatments. Conversely, HA cables were not observed with IL-1α treatment (Fig. 1D). Lower magnification images show the extent of cable formation by TM cells in a larger field of view (Fig. 1G). Although the data presented is from porcine TM cells, HA cables were

also formed by human TM cells in response to TNFα treatment suggesting that cable formation is species independent (not shown).

HAS mRNA levels in response to various treatments

It has been proposed that HA cables could be induced by modifying the activity of HAS genes.(Selbi et al., 2006b) Differential regulation of HAS genes may alter the synthesis rates of individual HA chains allowing for rearrangement into HA cables. Therefore, the effects of the various stimuli on HAS gene expression by TM cells was investigated by quantitative RT-PCR (Fig. 2). HAS1 gene expression was significantly increased after 12 hours of treatment with TNFα, IL-1α, and mechanical stretch (Fig. 2A). HAS1 mRNA levels remained significantly up-regulated at 24 hours with IL-1α treatment, but they were not sustained at later time points (24 and 48 hours) for TNFα and mechanical stretch. TGFβ2 did not significantly alter HAS1 gene expression at any of the time points tested. HAS2 mRNA levels were significantly increased approximately 3-fold in response to TNFα, TGFβ2, and IL-1α (Fig. 2B). However, each treatment exhibited different temporal responses: TNFα increased HAS2 mRNA at 12 and 24 hours, IL-1α effects were significant at 24 and 48 hours, while TGFβ2 increased HAS2 mRNA levels at all three time points tested. Conversely, HAS2 mRNA levels were almost unchanged in response to mechanical stretch at all three time points. HAS3 mRNA levels were not significantly altered in response to the cytokine treatments at any of the time points tested (Fig. 2C). Mechanical stretch significantly increased HAS3 mRNA levels approximately 3-fold at 12 hours, but this increase was not sustained at later time points. Thus, different external stimuli induced differential temporal responses of each HAS gene.

HA concentration

Previous studies have suggested that higher HA concentrations may influence cable formation.(Selbi et al., 2006b) To investigate HA levels in TM cells, a competitive ELISA assay was used to quantitate HA concentration in cell lysates and media from TM cells treated for 24 hours with the chosen stimuli (Fig. 3). In response to TNFα, TGFβ2 and IL-1α treatments, HA concentration in the media was significantly increased compared to the control, but there was no significant differences in HA concentration in the RIPA lysates. Conversely, for mechanical stretch, there was a significant decrease in HA concentration in the cell lysates, but no change detected in the media fraction.

Association of hyaladherins with HA cables in TM cells

Several hyaladherins, including TSG-6 and IαI, have been associated with HA cables in other cell types and these could promote cable formation by cross-linking individual HA chains into cables.(Day and de la Motte, 2005) The expression and distribution of TSG-6 and IαI in TM cells has not been previously studied. Therefore, we assessed the protein localization and levels of TSG-6 and the IαI/bikunin complex in TM cells.

IαI is a protein complex of the CS-substituted proteoglycan bikunin with two HCs.(Salier et al., 1996) In untreated control cells, IαI (green) diffusely labeled TM cells and there was little colocalization with HAbp (red) by confocal microscopy (Fig. 4A–C). In contrast, IαI colocalized with HAbp in long cellular protrusions and HA cables in TM cells treated for 48

hours with TNFα (Fig. 4D–F). The protein levels of bikunin in response to external stimuli were investigated by Western immunoblotting. Consistent with a previous report,(Sjoberg and Fries, 1992) bikunin was found in the media as a free form (42 kDa) and as a higher molecular weight complex with HCs (240 kDa). Bikunin levels were significantly increased in TM cells treated with TNFα, TGFβ2 and IL-1α for 48 hours (Fig. 4G). However, there was a significant decrease in protein levels of bikunin with mechanical stretch compared to control. In addition, a new band at approximately 52 kDa was observed in control cells cultured on the silicone membrane (right panel) compared with the control cultured on the rigid plastic surface (left panel). Densitometry of the 42 kDa and 240 kDa bands showed 20–40% increase in response to cytokines/growth factor treatments, and an approximately 50% decrease in response to mechanical stretch (Fig. 4H).

TSG-6 is a multifunctional protein that transfers HCs from IαI to HA chains.(Milner and Day, 2003) Therefore, we evaluated protein levels and distribution of TSG-6 in response to the various external stimuli. In untreated control cells (Fig. 5A–C), TSG-6 (green; Fig. 5A) showed a diffuse distribution with some patches of more intense immunostaining at the cell periphery. This TSG-6 staining did not colocalize with HAbp (red; Fig. 5B; merged image in Fig. 5C). However, TSG-6 was highly increased following TNFα treatment (Fig. 5D–F). There was a large increase in TSG-6 cellular staining (green; Fig. 5E) as well as apparent colocalization of TSG-6 with extracellular HAbp-labeled HA cables (arrows; red; Fig. 5D; merged image in Fig. 5F).

To quantitate this apparent increase in TSG-6 protein levels, Western immunoblotting was performed. The predicted molecular weight of TSG-6 is 35 kDa, but it can form a SDS-stable complex with HC1 or HC2 from IαI that is approximately 120 kDa.(Nagyeri et al., 2011; Sanggaard et al., 2010) A 80 kDa band was also detected in synovial fluid, which is thought to be a degradation product of the TSG-6•HC complex.(Nagyeri et al., 2011) In Western immunoblots of TM cell media, very little free TSG-6 (~39 kDa) was detected and the majority of TSG-6 synthesized by TM cells appeared to be complexed with HCs (120 kDa and 80 kDa degradation product; Fig. 5G). All cytokine and growth factor treatments increased TSG-6 levels, while mechanical stretch significantly decreased TSG-6 protein levels. The underlying substrata appeared to influence the composition of TSG-6 complexes because an additional band at approximately 100 kDa was enriched when TM cells were cultured on a silicone membrane compared to a rigid plastic surface. The 120 kDa and 100 kDa bands are consistent with TSG-6 complexed with HC2 and HC1, respectively.(Rugg et al., 2005) Densitometry of the Western immunoblots revealed a 30–50% increase in TNFα, TGFβ2 and IL-1α-treated cells, and an approximately 50% decrease in TSG-6 protein levels in response to mechanical stretch (Fig. 5H). The free TSG-6 band (~39 kDa) was not quantitated as it was too faint.

PolyI:C induction of HA cables

When applied exogenously to anterior segments in perfusion culture, TNFα increases outflow whereas TGFβ2 decreases outflow.(Bradley et al., 2000; Fleenor et al., 2006; Gottanka et al., 2004) Thus, stimuli that induce HA cable formation have opposite effects on outflow. We therefore investigated whether rearrangement of pericellular HA into cables

affected outflow. To do this, we applied polyinosinic:polycytidylic acid (polyI:C), which is a potent stimulator of HA cable formation,(de la Motte et al., 2003; Evanko et al., 2009) to cell culture and anterior segment perfusion organ culture. When TM cells were cultured for 24 hours in the presence of polyI:C, HA cable formation was induced (Fig. 6A, B). Porcine anterior segments were perfused with serum-free media until flow rates had stabilized. At time point 0, 10 μg/ml polyI:C was added and outflow was monitored for a further 71 hours (Fig. 6C). Although outflow rates increased marginally with polyI:C treatment, these were not significantly different from control anterior segments that were perfused with serum-free media alone. HAbp was used to label radial sections of control (Fig. 6D) and polyI:C-treated (Fig. 6E) porcine TM tissue. There was a slight increase in the fluorescence signal in polyI:C-treated eyes and the pattern was less punctate than the control TM. This distribution pattern is consistent with polyI:C-induced HA cable formation.

Discussion

In this study, we show that TM cells can form HA cable-like structures in response to several, but not all, stimuli that induce ECM remodeling and alter aqueous outflow resistance. TNFα, TGFβ2 and mechanical stretch induced HA cable formation, whereas IL-1α did not. In addition, we show that *HAS* gene expression, HA concentration, and levels of hyaladherins are differentially modified in response to TNFα, TGFβ2, IL-1α and mechanical stretch. A previous study detected HA cables in response to IL-1α treatment of epidermal keratinocytes and they showed that TNFα and IL-1α did not significantly affect HAS gene expression or HA concentration.(Jokela et al., 2008) Thus, responses to external stimuli are cell-specific and multiple mechanisms may exist that lead to tissue-specific formation of HA cables. Our perfusion experiments at physiological pressure indicated that rearrangement of pericellular HA into HA cables does not significantly affect outflow. However, this does not preclude the possibility that in other conditions, e.g. elevated pressure, that induction of HA cables may influence outflow rates.

The only apparent difference between stimuli that induce cable formation (TNFα, TGFβ2, mechanical stretch) and those that didn't (IL-1α) in TM cells was the activity of the HAS genes. At 12 hours, IL-1α increased the expression of HAS1 without altering the transcription of HAS2 or HAS3. However, at this time point, there were concomitant increases in HAS2 and HAS3 mRNA by TNFα and mechanical stretch, respectively. Our data therefore suggest that increases in HAS1 mRNA alone may prevent cable formation, while increases of HAS1 concomitant with HAS2 or HAS3 may induce cable formation. Previous studies have shown that over-expression of HAS3 induced HA cable formation and increased pericellular HA.(Selbi et al., 2006a; Selbi et al., 2006b) The authors proposed that low molecular weight HA produced by HAS3 may promote extension of longer HA chains. In addition, they showed that over-expression of recombinant HAS2 inhibited cable formation in renal proximal tubular epithelial cells.(Selbi et al., 2006a) This is opposite to our study where HAS2 mRNA expression was dramatically increased and HA cable formation was induced by TGFβ2 treatment. The reason for this apparent discrepancy between studies is not clear. The authors offered several reasons as to why cable formation did not occur in HAS2-overexpressed cells including concomitant increases in hyaluronidase activity that cleave extruded HA chains at the cell surface, competition for

UDP-sugars may attenuate HAS3-induced cable formation, or specific structural components present at the cell surface may be insufficient in HAS2-transfected cells. Induction of endogenous HAS2 by TGFβ2 treatment may not be subject to these restrictions. For instance, TGFβ2 may concomitantly induce expression of factors that promote cable formation and/or there may be no effect on hyaluronidase activity. Collectively, these studies show that precise regulation of each HAS gene is likely required in order to synthesize and build a unique tissue-specific ECM that allows cells to respond and adapt to specific responses. Future studies using *HAS*-specific gene knockdown or use of HAS over-expression vectors should elucidate the individual contributions of HAS genes to HA cable formation in TM cells.

HA concentration in the media increased with TNFα, TGFβ2, IL-1α treatment, but there was no change in the pericellular matrix. Conversely, mechanical stretch reduced HA concentration in the pericellular matrix and there was no significant difference in HA levels in the media. Furthermore, protein levels of TSG-6 and bikunin were increased by TNFα, TGFβ2, IL-1α treatment, but were reduced by mechanical stretch. HA concentration and levels of hyaladherins have been suggested to be determinants of cable formation,(Evanko et al., 2009) but our data suggests these are not critical regulators of cable formation by TM cells. A recent study showed that addition of recombinant TSG-6 alone did not induce cable formation.(Lauer et al., 2013) Our data are consistent with this study since TSG-6 was up-regulated by IL-1α, but this cytokine did not induce cable formation.

The structural configuration of HA cables in response to mechanical stretch appeared to be different than those formed by TNFα and TGFβ2 treatments by confocal microscopy. Cables induced by mechanical stretch appeared as alignment of multiple HAbp-labeled punctate dots, whereas cables formed by TNFα and TGFβ2 were more solid lines. Both patterns have been reported previously.(Evanko et al., 2009) The differences in distribution patterns may reflect accessibility of the HAbp link domain to binding sites on the HA cable due to occupation of sites by other HA binding proteins. Indeed, it was proposed that altering the conformation of HA may positively or negatively modulate the binding of hyaladherins. (Day and Prestwich, 2002) Alternatively, HAbp binding patterns may indicate differences in the composition of the cable due to altered contributions of individual HA chains contributed by HAS1, HAS2, or HAS3.

Treatments that promote cable formation also increase microvillus-like cell protrusions and HA cables may arise from the tips of these protrusions.(Kultti et al., 2006) TNFα treatment of TM cells causes a profound phenotypic change and there is an increase in membrane protrusions.(Kelley et al., 2007) In TM cells, these protrusions could aid HA cable formation. However, there is some debate as to the difference between HA cables and microvillus-like cell protrusions since there are no definitive criteria to distinguish one from the other.(Evanko et al., 2009) Thus, the extent of cellular involvement in the formation of HA cables remains unclear.

HA concentration in glaucomatous TM is significantly lower than age-matched TM. (Knepper et al., 1996a; Knepper et al., 1996b) Previously, we found that silencing the *HAS1* and *HAS2* genes reduced HA concentration and reduced outflow in human anterior

perfusion culture.(Keller et al., 2012b) A recent study showed that when HA concentrations are low, the pH of the tissue microenvironment is relatively high, which favors versican-HA complex formation.(Heng et al., 2008) Furthermore, we showed that reducing HA concentration also reduced versican protein levels.(Keller et al., 2012a) Thus, a feedback loop may ensue where decreased HA concentration leads to decreased versican and an ECM that is no longer capable of facilitating aqueous outflow through the TM. Decreased versican concentrations causing increased outflow resistance in human perfusion culture is consistent with this.(Keller et al., 2011) Mechanical stretch mimics the stretch/distortion placed on cells *in situ* by fluctuations in pressure and stimulates ECM remodeling by MMPs. Yet, the data shown here indicates that mechanical stretch decreases HA in the pericellular matrix, while we have previously shown that mechanical stretch reduces versican mRNA expression.(Keller et al., 2007) Thus, transient events that homeostatically regulate IOP and chronic events that lead to elevated IOP both appear to involve decreased HA concentration and versican levels. This supports our contention that the correct concentration of HA and versican in the TM is critical for maintaining aqueous outflow through the TM. The levels and activity of hyaluronidases also likely contribute to maintaining the correct HA concentration in the TM. Hyaluronidases cleave HA chains into smaller fragments that are endocytosed at the cell surface by receptors such as CD44, RHAMM and Toll-like receptors.(Harada and Takahashi, 2007) Activation of these receptors activates TM cellular signaling pathways. Future studies will elucidate the contribution of hyaluronidases to maintaining HA concentration and TM cellular function.

A somewhat unexpected result was the observation that the underlying tissue culture substrate may affect the identity of TSG-6•HC complexes. TSG-6•HC2 complexes were assembled on rigid plastic surfaces, while TGS-6•HC1complexes were additionally formed on silicone membranes. Moreover, a 52kDa band recognized by bikunin antibodies was detected when TM cells were grown on silicone substrates. The identity of this band is unknown at present. Although several studies have reported that hyaladherins cross-link HA, (Baranova et al., 2013; Baranova et al., 2011) this is the first study to report that tissue culture substrates may influence the composition of the IαI•TSG-6•HA complexes. The plastic and silicone surfaces not only differ in rigidity (Young's moduli of 2–4 GPa for plastic versus ~930 kPa for silicone), but also have differences in collagen coating, surface charge and protein binding capacity. Previous studies demonstrated that TM cells are sensitive to alterations in the topography of the underlying substrata (Russell et al., 2008) and substrate compliance (Schlunck et al., 2008), both of which influence expression of ECM components. Future studies utilizing substrates of defined stiffness and/or substrates with various ECM coatings should elucidate factors important for assembly of TSG-6•HC complexes and HA cable formation.

In summary, we studied the effect of various stimuli on the ability to induce HA cable formation by TM cells and correlated cable formation to factors thought to be important for their formation (Table 2). IL-1α treatment did not induce HA cables, but was found to increase HA concentration and levels of the hyaladherins, TSG-6 and IαI. Conversely, cable formation occurred in mechanically stretched TM cells even though HA concentration and hyaladherins levels were reduced. Our data therefore suggests that an imbalance of the

normal ratio of HA chains synthesized by HAS1, HAS2 and HAS3 is the most likely critical factor for HA cable induction in TM cells.

Acknowledgements

This study was supported by a NIH/NEI grant (EY019643), a Sybil B. Harrington special scholar award to KEK and an unrestricted grant to the Casey Eye Institute by Research to Prevent Blindness, New York, NY. We thank Dr Ted Acott for critical reading of the manuscript.

References

1. Acott TS, Kelley MJ, Keller KE, Vranka JA, Abu-Hassan DW, Li X, Aga M, Bradley JM. Intraocular pressure homeostasis: maintaining balance in a high-pressure environment. J Ocul Pharmacol Ther. 2014; 30:94–101. [PubMed: 24401029]
2. Baranova NS, Foulcer SJ, Briggs DC, Tilakaratna V, Enghild JJ, Milner CM, Day AJ, Richter RP. Inter-alpha-inhibitor impairs TSG-6-induced hyaluronan cross-linking. J Biol Chem. 2013; 288:29642–29653. [PubMed: 24005673]
3. Baranova NS, Nileback E, Haller FM, Briggs DC, Svedhem S, Day AJ, Richter RP. The inflammation-associated protein TSG-6 cross-links hyaluronan via hyaluronan-induced TSG-6 oligomers. J Biol Chem. 2011; 286:25675–25686. [PubMed: 21596748]
4. Barany EH, Scotchbrook S. Influence of testicular hyaluronidase on the resistance to flow through the angle of the anterior chamber. Acta Physiol Scand. 1954; 30:240–248. [PubMed: 13158098]
5. Bradley JM, Anderssohn AM, Colvis CM, Parshley DE, Zhu XH, Ruddat MS, Samples JR, Acott TS. Mediation of laser trabeculoplasty-induced matrix metalloproteinase expression by IL-1beta and TNFalpha. Invest Ophthalmol Vis Sci. 2000; 41:422–430. [PubMed: 10670472]
6. Bradley JM, Kelley MJ, Zhu X, Anderssohn AM, Alexander JP, Acott TS. Effects of mechanical stretching on trabecular matrix metalloproteinases. Invest Ophthalmol Vis Sci. 2001; 42:1505–1513. [PubMed: 11381054]
7. Bradley JM, Rose A, Kelley MJ, Chen Y, Song K, Acott TS. Interactions between Il-1 and TNF: their effects on trabecular meshwork cells. Invest Ophthalmol Vis Sci. 2006; 47 E-abstract #1865.
8. Day AJ, de la Motte CA. Hyaluronan cross-linking: a protective mechanism in inflammation? Trends Immunol. 2005; 26:637–643. [PubMed: 16214414]
9. Day AJ, Prestwich GD. Hyaluronan-binding proteins: tying up the giant. J Biol Chem. 2002; 277:4585–4588. [PubMed: 11717315]
10. de la Motte CA, Drazba JA. Viewing hyaluronan: imaging contributes to imagining new roles for this amazing matrix polymer. J Histochem Cytochem. 2011; 59:252–257. [PubMed: 21378279]
11. de la Motte CA, Hascall VC, Drazba J, Bandyopadhyay SK, Strong SA. Mononuclear leukocytes bind to specific hyaluronan structures on colon mucosal smooth muscle cells treated with polyinosinic acid:polycytidylic acid: inter-alpha-trypsin inhibitor is crucial to structure and function. Am J Pathol. 2003; 163:121–133. [PubMed: 12819017]
12. Evanko SP, Potter-Perigo S, Johnson PY, Wight TN. Organization of hyaluronan and versican in the extracellular matrix of human fibroblasts treated with the viral mimetic poly I:C. J Histochem Cytochem. 2009; 57:1041–1060. [PubMed: 19581629]
13. Fleenor DL, Shepard AR, Hellberg PE, Jacobson N, Pang IH, Clark AF. TGFbeta2-induced changes in human trabecular meshwork: implications for intraocular pressure. Invest Ophthalmol Vis Sci. 2006; 47:226–234. [PubMed: 16384967]
14. Francois J, Rabaey M, Neetens A. Perfusion studies on the outflow of aqueous humor in human eyes. AMA Arch Ophthalmol. 1956; 55:193–204. [PubMed: 13282544]
15. Gottanka J, Chan D, Eichhorn M, Lutjen-Drecoll E, Ethier CR. Effects of TGF-beta2 in perfused human eyes. Invest Ophthalmol Vis Sci. 2004; 45:153–158. [PubMed: 14691167]
16. Grant WM. Experimental aqueous perfusion in enucleated human eyes. Arch Ophthalmol. 1963; 69:783–801. [PubMed: 13949877]
17. Harada H, Takahashi M. CD44-dependent intracellular and extracellular catabolism of hyaluronic acid by hyaluronidase-1 and -2. J Biol Chem. 2007; 282:5597–5607. [PubMed: 17170110]

18. Hascall VC, Majors AK, De La Motte CA, Evanko SP, Wang A, Drazba JA, Strong SA, Wight TN. Intracellular hyaluronan: a new frontier for inflammation? Biochim Biophys Acta. 2004; 1673:3–12. [PubMed: 15238245]
19. Heng BC, Gribbon PM, Day AJ, Hardingham TE. Hyaluronan binding to link module of TSG-6 and to G1 domain of aggrecan is differently regulated by pH. J Biol Chem. 2008; 283:32294–32301. [PubMed: 18806261]
20. Hubbard WC, Johnson M, Gong H, Gabelt BT, Peterson JA, Sawhney R, Freddo T, Kaufman PL. Intraocular pressure and outflow facility are unchanged following acute and chronic intracameral chondroitinase ABC and hyaluronidase in monkeys. Exp Eye Res. 1997; 65:177–190. [PubMed: 9268586]
21. Inatani M, Tanihara H, Katsuta H, Honjo M, Kido N, Honda Y. Transforming growth factor-beta 2 levels in aqueous humor of glaucomatous eyes. Graefes Arch Clin Exp Ophthalmol. 2001; 239:109–113. [PubMed: 11372538]
22. Itano N, Sawai T, Yoshida M, Lenas P, Yamada Y, Imagawa M, Shinomura T, Hamaguchi M, Yoshida Y, Ohnuki Y, Miyauchi S, Spicer AP, McDonald JA, Kimata K. Three isoforms of mammalian hyaluronan synthases have distinct enzymatic properties. J Biol Chem. 1999; 274:25085–25092. [PubMed: 10455188]
23. Jokela TA, Lindgren A, Rilla K, Maytin E, Hascall VC, Tammi RH, Tammi MI. Induction of hyaluronan cables and monocyte adherence in epidermal keratinocytes. Connect Tissue Res. 2008; 49:115–119. [PubMed: 18661324]
24. Keller KE, Aga M, Bradley JM, Kelley MJ, Acott TS. Extracellular matrix turnover and outflow resistance. Exp Eye Res. 2009a; 88:676–682. [PubMed: 19087875]
25. Keller KE, Bradley JM, Acott TS. Differential effects of ADAMTS-1, -4, and -5 in the trabecular meshwork. Invest Ophthalmol Vis Sci. 2009b; 50:5769–5777. [PubMed: 19553617]
26. Keller KE, Bradley JM, Kelley MJ, Acott TS. Effects of modifiers of glycosaminoglycan biosynthesis on outflow facility in perfusion culture. Invest Ophthalmol Vis Sci. 2008; 49:2495–2505. [PubMed: 18515587]
27. Keller KE, Bradley JM, Vranka JA, Acott TS. Segmental versican expression in the trabecular meshwork and involvement in outflow facility. Invest Ophthalmol Vis Sci. 2011; 52:5049–5057. [PubMed: 21596823]
28. Keller KE, Kelley MJ, Acott TS. Extracellular matrix gene alternative splicing by trabecular meshwork cells in response to mechanical stretching. Invest Ophthalmol Vis Sci. 2007; 48:1164–1172. [PubMed: 17325160]
29. Keller KE, Sun YY, Vranka JA, Hayashi L, Acott TS. Inhibition of hyaluronan synthesis reduces versican and fibronectin levels in trabecular meshwork cells. PLoS One. 2012a; 7:e48523. [PubMed: 23139787]
30. Keller KE, Sun YY, Yang YF, Bradley JM, Acott TS. Perturbation of hyaluronan synthesis in the trabecular meshwork and the effects on outflow facility. Invest Ophthalmol Vis Sci. 2012b; 53:4616–4625. [PubMed: 22695958]
31. Kelley MJ, Rose AY, Song K, Chen Y, Bradley JM, Rookhuizen D, Acott TS. Synergism of TNF and IL-1 in the induction of matrix metalloproteinase-3 in trabecular meshwork. Invest Ophthalmol Vis Sci. 2007; 48:2634–2643. [PubMed: 17525194]
32. Knepper PA, Farbman AI, Telser AG. Exogenous hyaluronidases and degradation of hyaluronic acid in the rabbit eye. Invest Ophthalmol Vis Sci. 1984; 25:286–293. [PubMed: 6698747]
33. Knepper PA, Goossens W, Hvizd M, Palmberg PF. Glycosaminoglycans of the human trabecular meshwork in primary open-angle glaucoma. Invest Ophthalmol Vis Sci. 1996a; 37:1360–1367. [PubMed: 8641839]
34. Knepper PA, Goossens W, Palmberg PF. Glycosaminoglycan stratification of the juxtacanalicular tissue in normal and primary open-angle glaucoma. Invest Ophthalmol Vis Sci. 1996b; 37:2414–2425. [PubMed: 8933758]
35. Kultti A, Rilla K, Tiihonen R, Spicer AP, Tammi RH, Tammi MI. Hyaluronan synthesis induces microvillus-like cell surface protrusions. J Biol Chem. 2006; 281:15821–15828. [PubMed: 16595683]

36. Lauer ME, Cheng G, Swaidani S, Aronica MA, Weigel PH, Hascall VC. Tumor necrosis factor-stimulated gene-6 (TSG-6) amplifies hyaluronan synthesis by airway smooth muscle cells. J Biol Chem. 2013; 288:423–431. [PubMed: 23129777]
37. Lauer ME, Fulop C, Mukhopadhyay D, Comhair S, Erzurum SC, Hascall VC. Airway smooth muscle cells synthesize hyaluronan cable structures independent of inter-alpha-inhibitor heavy chain attachment. J Biol Chem. 2009; 284:5313–5323. [PubMed: 19075022]
38. Milner CM, Day AJ. TSG-6: a multifunctional protein associated with inflammation. J Cell Sci. 2003; 116:1863–1873. [PubMed: 12692188]
39. Milner CM, Higman VA, Day AJ. TSG-6: a pluripotent inflammatory mediator? Biochem Soc Trans. 2006; 34:446–450. [PubMed: 16709183]
40. Nagyeri G, Radacs M, Ghassemi-Nejad S, Tryniszewska B, Olasz K, Hutas G, Gyorfy Z, Hascall VC, Glant TT, Mikecz K. TSG-6 protein, a negative regulator of inflammatory arthritis, forms a ternary complex with murine mast cell tryptases and heparin. J Biol Chem. 2011; 286:23559–23569. [PubMed: 21566135]
41. Polansky JR, Weinreb RN, Baxter JD, Alvarado J. Human trabecular cells I. Establishment in tissue culture and growth characteristics. Invest Ophthalmol Vis Sci. 1979; 18:1043–1049. [PubMed: 383640]
42. Rugg MS, Willis AC, Mukhopadhyay D, Hascall VC, Fries E, Fulop C, Milner CM, Day AJ. Characterization of complexes formed between TSG-6 and inter-alpha-inhibitor that act as intermediates in the covalent transfer of heavy chains onto hyaluronan. J Biol Chem. 2005; 280:25674–25686. [PubMed: 15840581]
43. Russell P, Gasiorowski JZ, Nealy PF, Murphy CJ. Response of human trabecular meshwork cells to topographic cues on the nanoscale level. Invest Ophthalmol Vis Sci. 2008; 49:629–635. [PubMed: 18235008]
44. Salier JP, Rouet P, Raguenez G, Daveau M. The inter-alpha-inhibitor family: from structure to regulation. Biochem J. 1996; 315(Pt 1):1–9. [PubMed: 8670091]
45. Sanggaard KW, Hansen L, Scavenius C, Wisniewski HG, Kristensen T, Thogersen IB, Enghild JJ. Evolutionary conservation of heavy chain protein transfer between glycosaminoglycans. Biochim Biophys Acta. 2010; 1804:1011–1019. [PubMed: 20100602]
46. Sawaguchi S, Lam TT, Yue BY, Tso MO. Effects of glycosaminoglycan-degrading enzymes on bovine trabecular meshwork in organ culture. J Glaucoma. 1993; 2:80–86. [PubMed: 19920491]
47. Schlunck G, Han H, Wecker T, Kampik D, Meyer-ter-Vehn T, Grehn F. Substrate rigidity modulates cell matrix interactions and protein expression in human trabecular meshwork cells. Invest Ophthalmol Vis Sci. 2008; 49:262–269. [PubMed: 18172101]
48. Selbi W, Day AJ, Rugg MS, Fulop C, de la Motte CA, Bowen T, Hascall VC, Phillips AO. Overexpression of hyaluronan synthase 2 alters hyaluronan distribution and function in proximal tubular epithelial cells. J Am Soc Nephrol. 2006a; 17:1553–1567. [PubMed: 16687630]
49. Selbi W, de la Motte CA, Hascall VC, Day AJ, Bowen T, Phillips AO. Characterization of hyaluronan cable structure and function in renal proximal tubular epithelial cells. Kidney Int. 2006b; 70:1287–1295. [PubMed: 16900089]
50. Sjoberg EM, Fries E. Biosynthesis of bikunin (urinary trypsin inhibitor) in rat hepatocytes. Arch Biochem Biophys. 1992; 295:217–222. [PubMed: 1586149]
51. Stamer WD, Acott TS. Current understanding of conventional outflow dysfunction in glaucoma. Curr Opin Ophthalmol. 2012; 23:135–143. [PubMed: 22262082]
52. Stamer WD, Seftor RE, Williams SK, Samaha HA, Snyder RW. Isolation and culture of human trabecular meshwork cells by extracellular matrix digestion. Curr Eye Res. 1995; 14:611–617. [PubMed: 7587308]
53. Stern R, Asari AA, Sugahara KN. Hyaluronan fragments: an information-rich system. Eur J Cell Biol. 2006; 85:699–715. [PubMed: 16822580]
54. Toole BP. Hyaluronan and its binding proteins, the hyaladherins. Curr Opin Cell Biol. 1990; 2:839–844. [PubMed: 1707285]
55. Toole BP. Hyaluronan: from extracellular glue to pericellular cue. Nat Rev Cancer. 2004; 4:528–539. [PubMed: 15229478]

56. Tripathi RC, Li J, Chan WF, Tripathi BJ. Aqueous humor in glaucomatous eyes contains an increased level of TGF-beta 2. Exp Eye Res. 1994; 59:723–727. [PubMed: 7698265]

57. Zhao M, Yoneda M, Ohashi Y, Kurono S, Iwata H, Ohnuki Y, Kimata K. Evidence for the covalent binding of SHAP, heavy chains of inter-alpha-trypsin inhibitor, to hyaluronan. J Biol Chem. 1995; 270:26657–26663. [PubMed: 7592891]

58. Zhuo L, Hascall VC, Kimata K. Inter-alpha-trypsin inhibitor, a covalent protein-glycosaminoglycan-protein complex. J Biol Chem. 2004; 279:38079–38082. [PubMed: 15151994]

- TNFα, TGFβ2 and mechanical stretch, but not IL-1α, induced hyaluronan cables
- The ratio of chains produced by each HAS gene is critical for HA cable formation
- Underlying tissue culture substrate affects composition of IαI•TSG-6•HA complexes
- Rearrangement of pericellular HA into cables does not influence outflow resistance

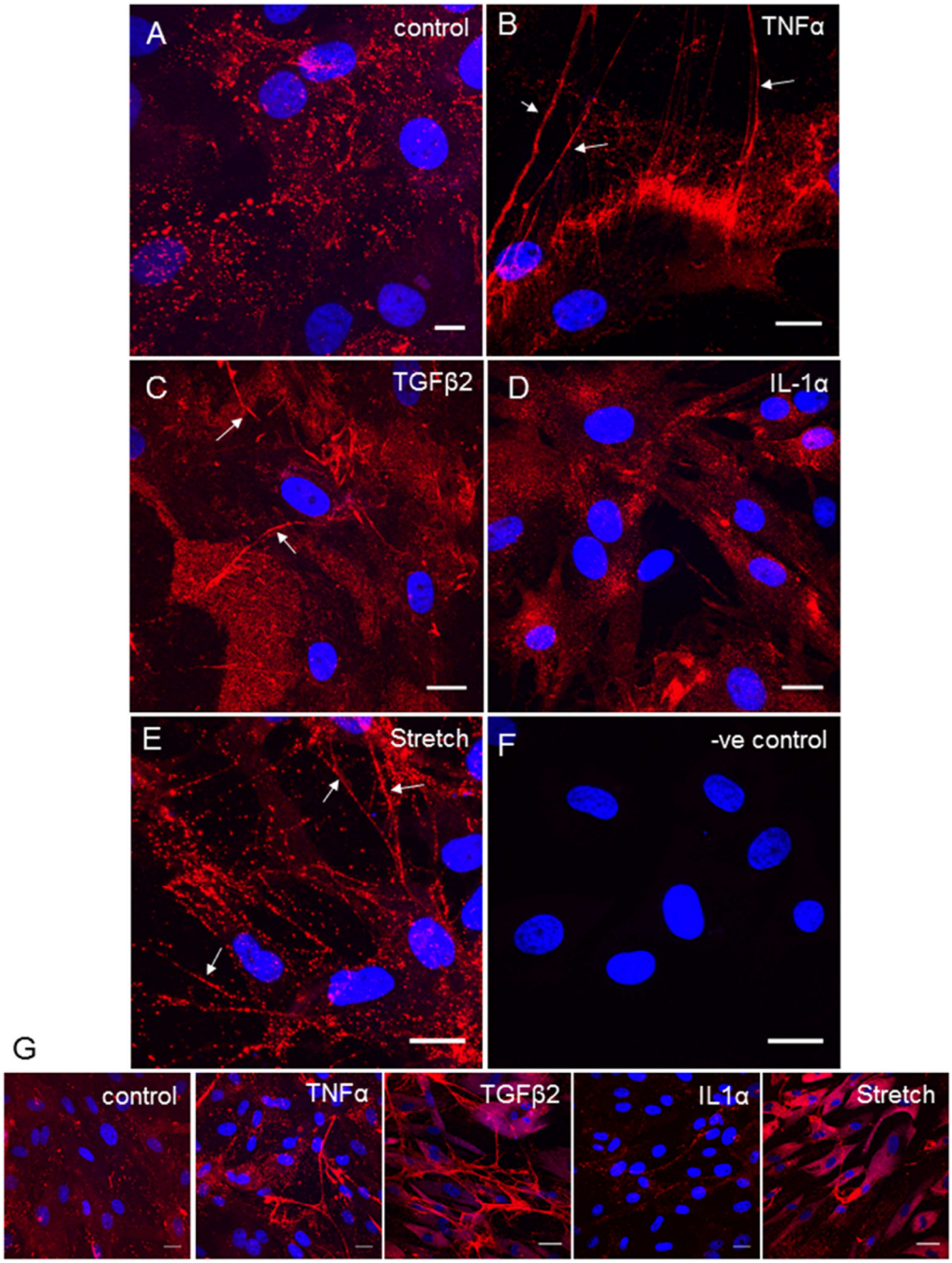

Figure 1. HA cable formation by TM cells

Biotinylated hyaluronic acid binding protein (bHAbp) and confocal microscopy was used to detect HA configuration in untreated control TM cell cultures (A), or in cells treated for 3 days with 10 ng/ml TNFα (B), 5 ng/ml TGFβ2 (C), 10 ng/ml IL-1α (D) or mechanical stretch (E). A control with no bHAbp staining is shown (F). Lower magnification images of control and treated cells to show cable formation in a larger field of view (G). DAPI was used to stain the nuclei (Blue). Scale bars = 20 μm.

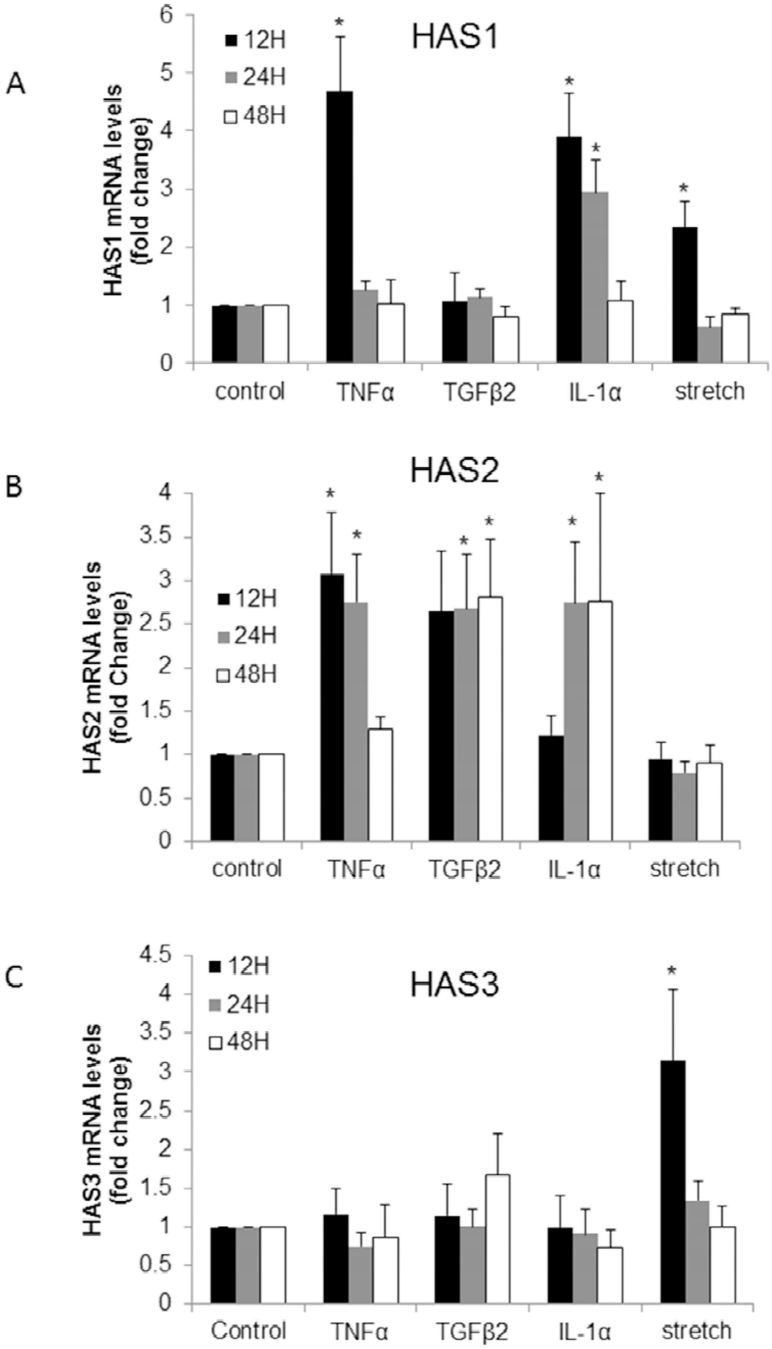

Figure 2. HAS mRNA levels in TM cells in response to various agents

Quantitative RT-PCR was used to measure *HAS1* (A), *HAS2* (B) and *HAS3* (C) mRNA levels in TM cells treated for 12, 24, and 48 hours with 10 ng/ml TNFα, 5 ng/ml TGFβ2, 10 ng/ml IL-1α or mechanical stretch. Results were normalized for 18S RNA and are presented as fold-change of untreated control cells. * $p<0.04$ by ANOVA; n= 3 to 7.

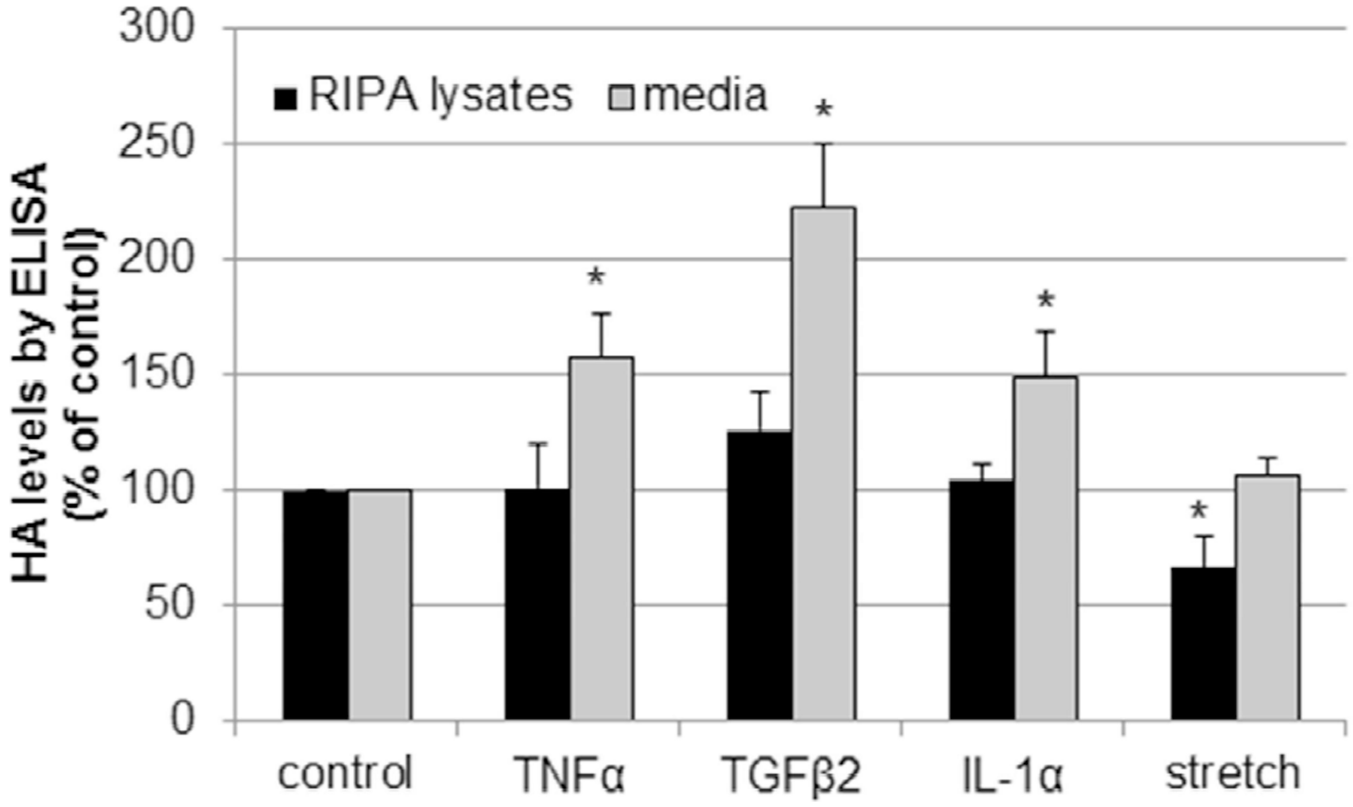

Figure 3. Measurement of HA concentration by ELISA

TM cells were treated for 24 hours with TNFα, IL-1α or TGFβ2 or mechanical stretch and the HA levels in serum-free media and RIPA cell extracts was quantitated by a competitive ELISA assay. HA levels in RIPA lysates and media are presented as a percentage of the control. N=6; *, P<0.05 by ANOVA.

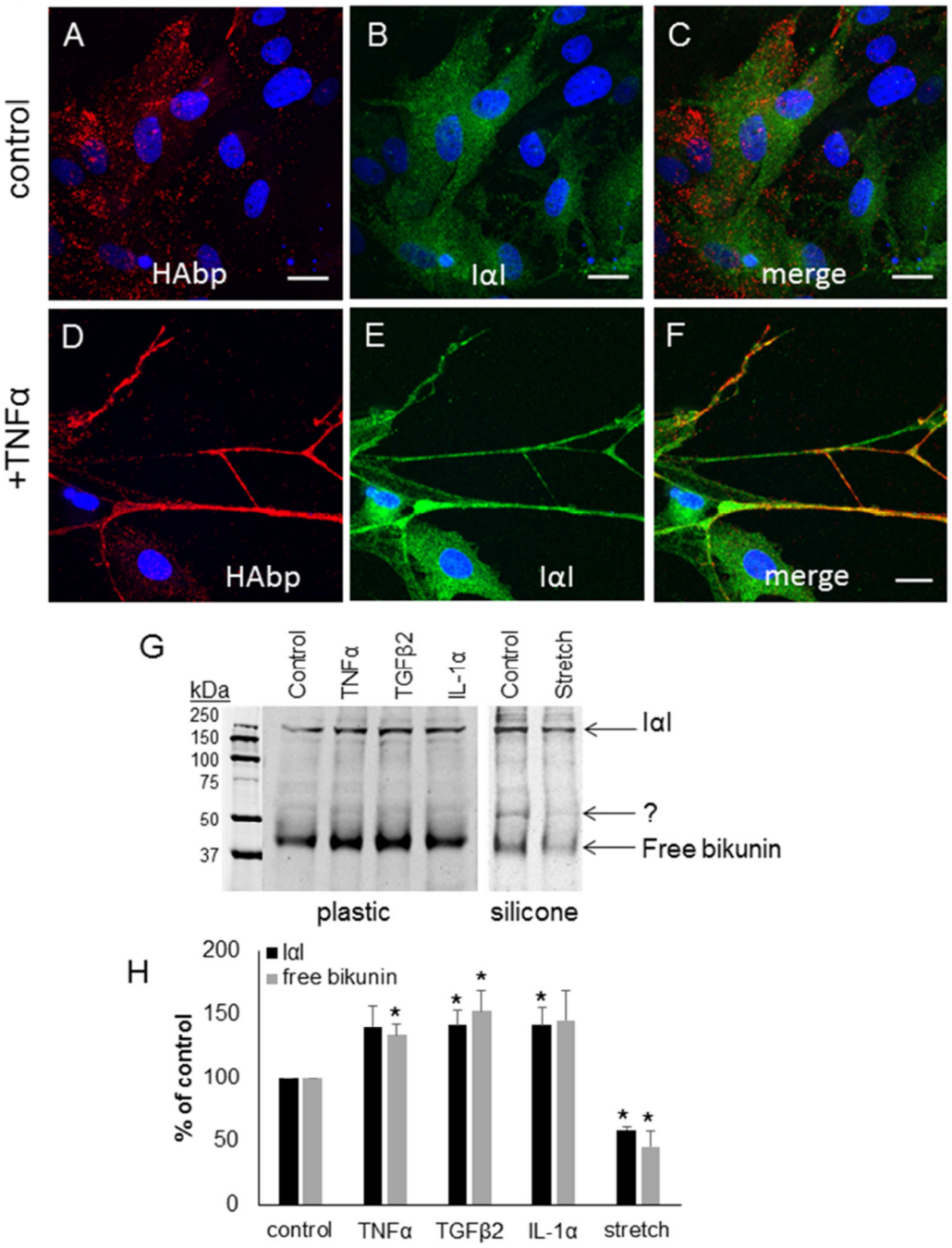

Figure 4. Bikunin and Inter-α-Inhibitor in TM cells

Inter-α-inhibitor (green) was colocalized with HAbp (red) in control TM cells (A–C) or in TM cells treated for 3 days with TNFα (D–F). Merged images are shown (C, F). Confocal acquisition settings were maintained between untreated and TNFα-treated TM cells. DAPI was used to stain the nuclei (blue). Scale bars = 20 μm. (G) Western immunoblots of bikunin in media from untreated cells (control) and following treatment for 48 hours with TNFα, TGFβ2, IL-1α and mechanical stretch. The positions of free bikunin (42 kDa) and bikunin complexed with HCs to form IαI (240 kDa) are indicated. Equal amounts of protein were

loaded into each lane. The cells on the left panel were cultured on plastic, whereas the cells in the right panel were cultured on collagen-coated silicone membrane. (H) Densitometry of bikunin bands are presented as a percentage of untreated control cells. N=3.* $p < 0.05$ by ANOVA.

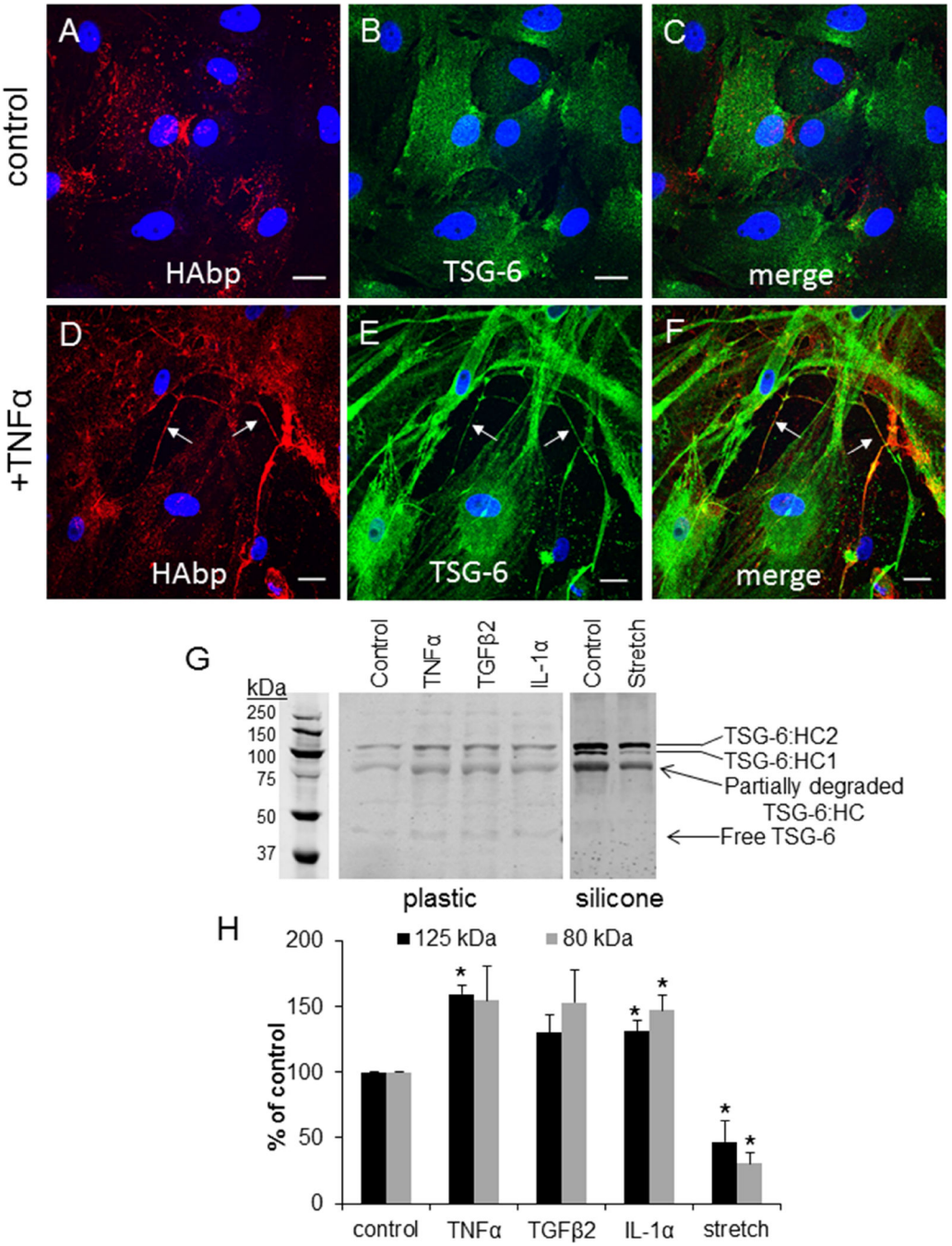

Figure 5. TSG-6 in TM cells

TSG-6 (green) was colocalized with HAbp (red) in untreated PTM cells (A–C) and in cells treated for 3 days with TNFα (D–F). Merged images are shown (C, F). Confocal acquisition settings were maintained between untreated control and TNFα-treated TM cells. DAPI was used to stain the nuclei (blue). Scale bars = 20 μm. (G) Western immunoblots of TSG-6 in media in untreated and following treatment for 48 hours with TNFα, TGFβ2, IL-1α and mechanical stretch. The positions of TSG-6 complexed with HCs (~120 kDa) and a degradation product (80 kDa) are indicated. Equal amounts of protein were loaded into each

lane for media. The cells on the left panel were cultured on plastic, whereas the cells in the right panel were cultured on collagen-coated silicone membrane. (I) Densitometry of TSG-6 levels in untreated and treated TM cells. N=3. * $p < 0.05$ by ANOVA.

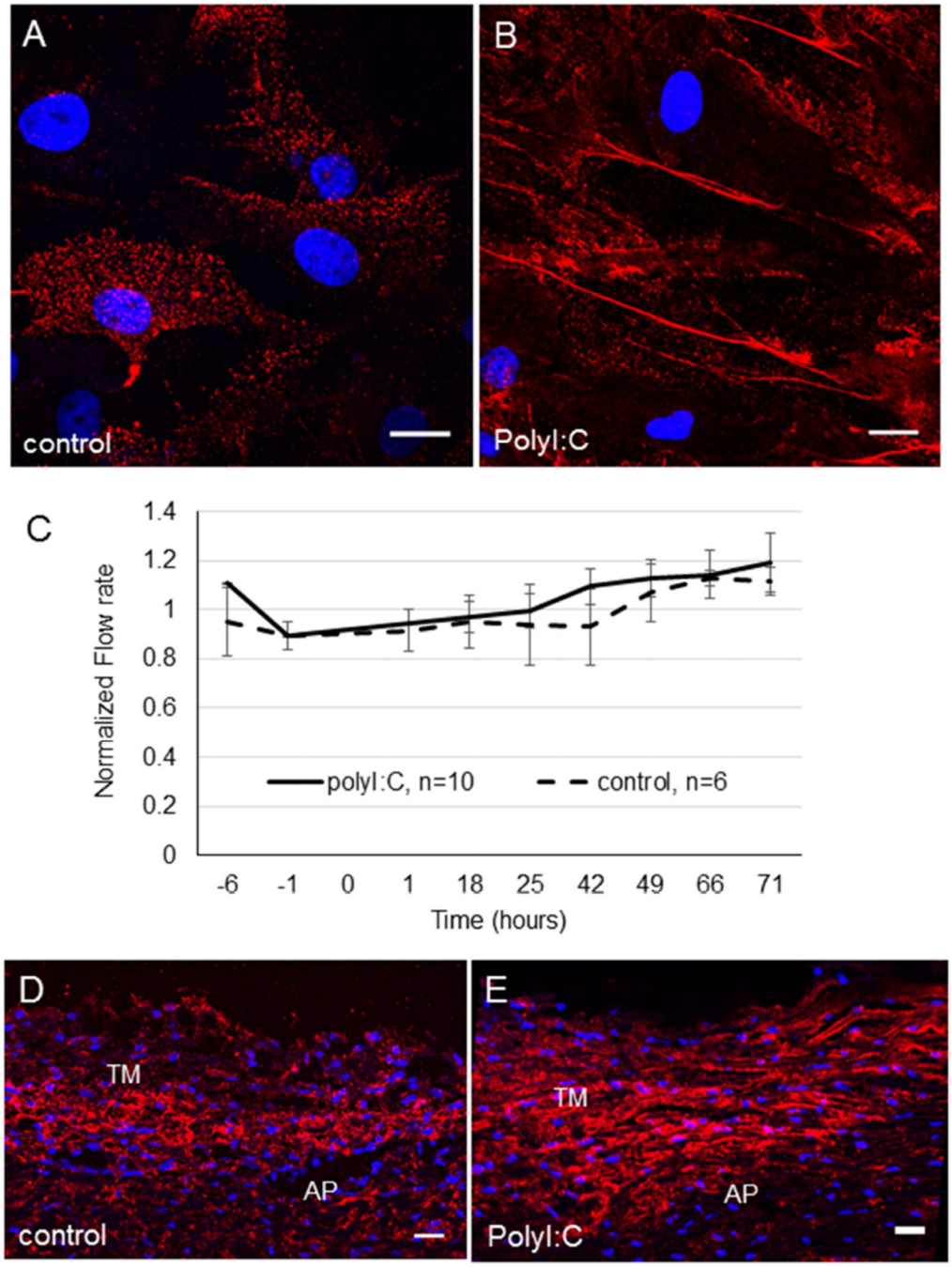

Figure 6. Induction of HA cables by polyI:C and the effect of polyI:C on outflow rates in porcine anterior segment perfusion culture

TM cells in culture were (A) untreated (control) or (B) treated with 10 μg/ml polyI:C in PBS for 24 hours. HAbp was used to detect HA cable formation. DAPI was used to stain the nuclei (blue). Scale bars = 20 μm. (C) Porcine anterior segments were perfused with serum-free media. At time point 0, 10 μg/ml polyI:C in PBS was applied. Control anterior segments were untreated. Data shows the average flow rate ± standard error of the mean. N=10 for polyI:C; n=6 for control. HAbp staining of control porcine TM tissue (D) and polyI:C-

treated TM (E). The cornea is positioned to the right in each image. AP = aqueous plexus. DAPI was used to stain the nuclei (blue). Scale bars = 20 μm.

Table 1

HAS gene primers for quantitative RT-PCR.

Gene	Forward (5'-3')	Reverse (5'-3')	Product size (bp)
HAS1	ACTGGGTAGCCTTCAATGTGGA	TACCAGGCCTCAAGAAACTGCT	121
HAS2	ATCCTCCTGGGTGGTGTGATTT	TTCCGCCTGCCACACTTATTGA	164
HAS3	TCCTACTTTGGCTGTGTGCAGT	TCCAGAGGTGGTGCTTATGGAA	313

Table 2

Summary of the data.

Treatment	HA cable formation	HAS mRNA (time in hours)	HA conc.	Bikunin	TSG6	Outflow rates
TNFα	Yes	HAS1 – 12↑ HAS2 – 12↑, 24↑	↑	↑	↑	↑*
TGFβ2	Yes	HAS2 – 12↑, 24↑, 48↑	↑	↑	↑	↓**
IL-1α	No	HAS1 – 12↑, 24↑ HAS2 – 24↑, 48↑	↑	↑	↑	↑*
Mechanical stretch	Yes	HAS1 – 12↑ HAS3 – 12↑	↓	↓	↓	↑***

* (Bradley et al., 2000);

** (Fleenor et al., 2006; Gottanka et al., 2004);

*** (Bradley et al., 2001).